Title

Analyzing Nasal Septal Deviations to Develop a New Classification System



Journal

Facial Plastic Surgery & Aesthetic Medicine, 16(3)

ISSN

2689-3614

Authors

Lin, Jonathan K

Wheatley, Francis C

Handwerker, Jason

et al.

Publication Date

2014-05-01

DOI

10.1001/jamafacial.2013.2480

Published in final edited form as:
*JAMA Facial Plast Surg*. 2014 ; 16(3): 183–187. doi:10.1001/jamafacial.2013.2480.

# Analyzing Nasal Septal Deviations to Develop a New Classification System:

## A Computed Tomography Study Using MATLAB and OsiriX

**Jonathan K. Lin, BSc**, **Francis C. Wheatley**, **Jason Handwerker, MD**, **Norman J. Harris, MD**, and **Brian J. F. Wong, MD, PhD**

Beckman Laser Institute and Medical Clinic, University of California, Irvine (Lin, Wheatley, Wong); Department of Otolaryngology–Head and Neck Surgery, University of California, Irvine Medical Center, Irvine (Lin, Handwerker, Harris, Wong); Department of Radiological Sciences, University of California, Irvine Medical Center, Irvine (Handwerker); Department of Biomedical Engineering, University of California, Irvine (Wong)

## Abstract

**IMPORTANCE—**Accurately characterizing nasal septal deviations is valuable for surgical planning, classifying nasal septal deviations, providing a means to accurately perform outcomes research, and understanding the causes of chronic conditions.

**OBJECTIVE—**To determine and quantify regions of septal deformity that can be used to develop a comprehensive classification system.

**DESIGN, SETTING, AND PARTICIPANTS—**A retrospective case series study was conducted at an academic tertiary care hospital. Sixty-four participants were selected based on a convenience sample of computed tomography (CT) scans of the paranasal sinuses and midface available between June 29, 2011, and August 16, 2012. Exclusion criteria consisted of incomplete or inadequate CT series. The most recent CT scans were chosen for analyses regardless of the indication for imaging. Digital Imaging and Communications in Medicine format bitmap file–formatted data were obtained and analyzed using MATLAB and OsiriX. The line to curve ratio, deviation area, and root mean square (RMS) values of the septal contour vs the ideal straight septum fit were calculated. Analysis was performed to detect significant differences ($P < .05$) using the 3 measures.



Corresponding Author: Brian J. F. Wong, MD, PhD, Beckman Laser Institute and Medical Clinic, University of California, Irvine, 1002 Health Sciences Rd E, Irvine, CA 92617 (bjwong@uci.edu).

**Conflict of Interest Disclosures:** None reported.

**Additional Contributions:** Naveen Bhandarkar, MD, Department of Otolaryngology–Head and Neck Surgery, University of California, Irvine, provided helpful discussions.

**Author Contributions:** Messrs Lin and Wheatley had full access to all the data in the study and take responsibility for the integrity of the data and the accuracy of the data analysis.
*Study concept and design:* All authors. *Acquisition of data:* Lin, Wheatley.
*Analysis and interpretation of data:* All authors. *Drafting of the manuscript:* Lin, Wong.
*Critical revision of the manuscript for important intellectual content:* All authors.
*Statistical analysis:* Lin, Wheatley.
*Administrative, technical, or material support:* Lin, Wheatley, Handwerker, Wong.
*Study supervision:* Harris, Wong.

**MAIN OUTCOMES AND MEASURES—**Quantitative analysis of nasal septal deviation.

**RESULTS—**The population consisted of 50 male and 14 female patients aged 3 to 83 years (mean, 42 years). Mean line to curve ratios, areas, and RMS values were highest in contours that intersected the perpendicular plate–vomer junction, with a mean line to curve ratio of 1.04 and mean deviated area of 627.16 arbitrary units ($P = .02$). Maximal deviation areas were also seen midway from the perpendicular plate–vomer junction to the nasal spine with a mean area of 577.31 arbitrary units ($P = .01$). The RMS values were significantly elevated along the crista galli and perpendicular plate–vomer junction ($P < .05$).

**CONCLUSIONS AND RELEVANCE—**Maximum septal deviation is seen at the perpendicular plate–vomer junction and in the regions near the crista galli and anterior nasal spine. Deviation area and RMS values are important measures to characterize septal deviations. Understanding septal deviations can aid in developing a functional classification system of nasal septal deviations for clinical use and a means to better record and compare surgical outcomes.

**LEVEL OF EVIDENCE—**NA.

A comprehensive analysis of the nasal septum is important for surgical planning and documentation. In addition, a reliable classification system can improve communication among surgeons. There is no widely accepted classification system for septal deformities that is able to quantitatively measure and characterize the nature of the deviation. In the literature[1,2] there are limited reports of efforts to quantitatively analyze septal deviations. The lack of descriptive and quantitative measures for septal deviations presents a challenge to surgeons who seek to objectively measure or gauge severity and postoperative surgical outcomes as well as correlate radiologic images with clinical findings and patient-reported outcome measures. Recent studies[3] have also shown that different types of septal deviation affect the likelihood of successful surgical outcomes. Accordingly, characterizing septal deviations is the first step in developing a classification system. The objectives of this study were to analyze septal deviations and to develop a method to quantitatively describe the curvature, extent of deviation, and often complex shape of a nasal septum using computed tomography (CT) scans and image processing software.

## Methods

### Patients and Image Selection

Images from 64 patients who underwent CT scans of the mid-face and paranasal sinuses were selected at random from a database of scans performed between June 29, 2011, and August 16, 2012, at the University of California, Irvine Medical Center. This study was conducted under the review and approval of the institutional review board of the University of California, Irvine, in accordance with their guidelines. Patients provided written informed consent. Images were obtained from patients undergoing CT scans for indications including sinusitis, trauma, and other preoperative evaluations. All available cases were included regardless of the presence of fractures, the availability of radiologist documentation, or whether they were performed for acute trauma. Image sections were 1 mm thick (iCT 256 scanner; Philips). The patient demographics were characterized on the basis of age and sex. The mean age was 42 years (range, 3–83 years); the sample included 50 males and 14

females. Images with significant motion artifact or patient head rotation precluding image processing were excluded from the study.

## Image Analysis

The Digital Imaging and Communications in Medicine format bitmap file–formatted CT images were imported (OsiriX; Pixmeo). A 2-dimensional orthogonal viewing feature was used to find coronal and axial images. Contour plots of the septum were generated, and septal profiles were generated at 7 specific regions. These regions were selected on the basis of detailed analysis of multiple images with highly experienced senior surgeons and clinical faculty (N.J.H. and B.J.F.W.) in the Department of Otolaryngology–Head and Neck Surgery. The selected points are easily identified on CT imaging and represent clinically relevant regions. As shown in Figure 1, a sagittal section was used to determine where to analyze the corresponding axial and coronal images based on the predefined points. Points selected included the perpendicular plate of ethmoid bone and vomer bone junction, nasal spine, nasal bone, crista galli, and mid-distance between the perpendicular plate–vomer (PPV) junction and nasal spine. Selected images were imported into MATLAB (MathWorks; http://www.mathworks.com), and a straight septum was simulated for each contour. The software automatically created this straight septum after selection of start and end points. These points remained consistent across images. Points were selected along the actual septum, and the true septal contour was fit to a piecewise cubic hermite interpolating polynomial. The length of the true septal contour was then compared with the ideal septal contour (straight). The line to curve ratios, deviation area, and root mean square (RMS) values of the septal contour vs the straight septum fit were calculated for each image analyzed. First, we defined the line to curve ratio (dimensionless) as the length of the curved or actual septum over the length of a theoretical straight line representing a perfectly straight septum. This measure has been shown[2] to be effective in comparing septal deviation across populations. Second, we defined the deviation area as the area in arbitrary units (AU) based on the pixel area spanning the actual curved septum and the theoretical straight septum. Finally, the RMS value was calculated; RMS values are widely used in engineering, physics, and audiology to represent the mean amplitude of a deviation from baseline in structures resembling a waveform. The RMS is especially useful when deviations project from both sides of the baseline with varying amplitudes and can provide a measure of the overall mean amplitude across an entire segment.[4] The RMS is calculated by squaring both positive and negative deflections from baseline, calculating the mean, and finally calculating the square root to rescale the data. Thus, the RMS indicates the mean amplitude of deviation along the septum with the theoretical straight septum set as the baseline. Figure 2 shows a sample output from MATLAB indicating that the deviation area is measured by calculating the area between the septum deviation and the theoretical straight line. Additional information provided includes the number of points the user selected and the number of deflections across midline. The code exports the data into a spreadsheet format.

## Statistical Analysis

Analysis was performed to detect significant differences ($P < .05$) using 3 factors: differences in the line to curve ratios, area, and RMS values of the septal contour vs the straight septum fit, which were calculated and compared based on location along the septum.

A 1-way analysis of variance was conducted to compare means and detect differences between variables dependent on location. Data were separated into 7 groups based on the 7 clinically significant locations along the septum for which the 3 variables were analyzed. A Levene statistic was performed and found to be significant, indicating non-homogeneous variances. Thus, the Tamhane T2 post hoc test was performed to detect differences between groups more conservatively, adjusting for unequal variances and achieving a smaller false-positive rate.

## Results

The final study population satisfying the inclusion criteria consisted of 50 male and 14 female patients aged 3 to 83 years (mean, 42 years). Statistically significant differences were seen in each of the 3 variables used to classify septal deviation. Mean line to curve ratios, areas, and RMS values were highest in contours that intersected the PPV junction, indicating this as the region where deformity was most often identified. As shown in Figure 3, the coronal region through this junction had a mean line to curve ratio and RMS value of 1.04 and 2.98, respectively. In the axial plane, the PPV junction had a mean RMS value and deviated area of 4.03 and 627.16 AU, respectively, again significantly elevated ($P = .02$). Maximum deviation areas and RMS values were also seen midway from the PPV junction to the nasal spine with a mean area of 577.31 AU and a mean RMS value of 3.58 ($P = .01$). The RMS values were significantly elevated along the crista galli, with a mean value of 2.78 ($P = .02$). Figure 3 shows an anatomic representation of regions where maximum deviation was seen. The PPV junction (A2/C4), the region inferior to the crista galli (C3), and the region superior to the anterior nasal spine (A3) represented the most deviated regions of the septum as measured by the deviation area and the RMS value.

## Discussion

Others have attempted the classification and quantification of nasal septal deviations. Mladina[5] characterized septal deviations according to 7 patterns of deviation along various axes, a system that was modified by Rao et al[6] to provide additional structural information. Guyuron et al[7] used a 6-tiered system based on a C- or S-shaped septum as viewed from multiple orientations surgically. One of the challenges with these classification methods is the limited ability to precisely localize areas of deformity. Buyukertan et al[1] were able to use CT to divide the nasal septum into 10 areas of interest and to quantify each segment for deformity. Similarly, Jin and Lee[8] divided the septum into 6 quadrants in 2 dimensions to qualitatively describe deformities at each location. In an effort to include abnormalities involved in septal deviation, Baumann and Baumann[9] used a classification system based on septal geometry as well as concomitant turbinate abnormality. Most recently, Reitzen et al,[2] in their study to compare septal deviation in an adult vs pediatric population, described a CT-based system to quantify the degree of deviation along a standardized set of points based on anatomic markers. Their line to curve ratio measure was replicated in the present study to provide a basis for comparison.

A challenge remains with respect to providing reliable and consistent methods for surgeons to characterize septal deviations for preoperative or postoperative evaluation when a CT

scan is available. Figure 3 illustrates a limitation of the line to curve ratio for identifying key regions of nasal septum deviation. In the 7 defined regions, the line to curve ratio identified only the PPV junction as a statistically significant region of deviation. In contrast, the deviation area and RMS values identified other regions as being deviated and thus may provide improved sensitivity for semiautomatically identifying areas of deviation. The deviation area and RMS values correlated well with each other. In 2 of the 4 regions found to have statistically significant increased deviation by RMS values, deviation area measurements were also significant ($P < .05$). The 2 other regions also showed increased measurements of deviation area, although not statistically significant. It is likely that these 2 variables would also identify statistically significant differences given a larger sample size. In our study, the regions of the septum near the PPV junction, the anterior nasal spine, and the crista galli saw the highest areas of deviation. Deformities at the PPV junction are common and surgically challenging. At the anterior septal angle, caudal septal deviations and deviations through Little's area are often found. The deviations in the region of the crista galli must be interpreted with respect to the plane we defined as intersecting this fixed bony anatomic landmark and likely represent deformity along the dorsal aspect of the perpendicular plate extending toward the keystone region.

These morphometric findings correlate well with those seen in previous studies,[1] with the exception of the area near the crista galli, with our study being the first to see significant deviation in that region. As in previous CT-based studies,[1] the caudal septum was not directly analyzed because it was not readily or reliably visible on all CT images. Caudal septal deviations of even 1 mm can impair airflow, and these small deviations would be difficult to measure given the limited resolution of CT. The 7 points we defined for analysis were based on surveying experienced surgeons for relevant clinical landmarks that describe specific anatomic points easily visible on CT.

The selected points through which image sections were generated placed a focus on bony landmarks identified on virtually any CT scan. However, relying on these reproducible registry points creates limits with respect to being able to fully characterize deviations most prevalent within the quadrangular cartilage alone; accordingly, more research is needed. Future studies should examine the relationship between bony deformations on cartilage shape and curvature, although this form of topologic analysis is challenging and eludes ready quantitative description. Ultimately, structural deformities must be compared with symptoms and patient-reported outcome measures. One theoretical concern with measuring the deviation area is that it may correlate with stature and hence overestimate or underestimate the degree of septal deformation. However, we did not witness significant increases in variability of the deviated area measure when compared with unitless measures, such as the line to curve ratio or RMS value (Figure 3). Unfortunately, CT images are not usually obtained for most patients undergoing septoplasty or septorhinoplasty surgery. Similarly, radiation exposure associated with using CT as an evaluation tool is a persistent concern precluding its routine use as a staging technology. Nonetheless, using CT data and a visualization environment such as OsiriX provides investigators with a pool of virtual study patients that can be examined and reexamined as deviation criteria and taxonomy are iteratively refined and developed. The software used can also affect the ability to acquire

clinically accurate images for analysis. Here, we used the freeware version of a medical image processing software. Similar medical image processing software allows volumetric rendering to be performed to analyze soft-tissue structures in addition to bony structures seen more readily on CT. The present study has some of the same limitations as in previous studies, including image distortion and insufficient resolution to visualize specific structures. However, many of the features used in previously reported[5–7,9,10] septal deviation classification systems were readily visualized and observed using the virtual endoscopy feature, thus pointing to the ability of a classification system to incorporate both data obtained through CT analysis and virtual endoscopy findings.

Having quantitative measures that describe the deformation and often complex nature of a deviated septum, we sought to provide a tool for surgeons to evaluate the septum preoperatively and potentially also identify changes postoperatively. Future studies would look for correlations between the factors measured here with patient or clinician evaluations based on physical examination or endoscopic images. Using the CT analysis tools, we were able to perform detailed analysis that would be challenging with traditional CT software. The detailed steps and measures performed in this study may be the first toward designing a practical system that can be used by clinicians in the office setting. This analysis, performed on existing CT scans, will provide information on the location and degree of septal deformities and their prevalence and ideally lead to a comprehensive classification system, perhaps using a point-based system based on our findings.

## Conclusions

Our study identified a quantitative method of analyzing septal deformities that is the first step toward developing a comprehensive classification system to describe the various types of septal deviation. Using these 3 measures—line to curve ratio, deviation area, and RMS value—we found that the regions surrounding the PPV junction, anterior nasal spine, and crista galli represented the highest areas of deviation in our study population. We showed that deviation area and RMS values might be more sensitive at identifying areas of septal deviation compared with previously used measurements. In the future, combining our CT-based approach with virtual endoscopy analysis or physical examination findings may contribute to a practical classification system for nasal septal deviations. In addition to its educational and research applications, such a system can be used by practicing clinicians to evaluate patients with nasal septal abnormalities before and after surgery.

## References

1. Buyukertan M, Keklikoglu N, Kokten G. A morphometric consideration of nasal septal deviations by people with paranasal complaints: a computed tomography study. Rhinology. 2003; 41(1):21–24. [PubMed: 12677736]
2. Reitzen SD, Chung W, Shah AR. Nasal septal deviation in the pediatric and adult populations. Ear Nose Throat J. 2011; 90(3):112–115. [PubMed: 21412740]
3. Cho GS, Jang YJ. Deviated nose correction: different outcomes according to the deviation type. Laryngoscope. 2013; 123(5):1136–1142. [PubMed: 23532668]
4. Gelfand, SA. Essentials of Audiology. New York, NY: Thieme Medical Publishers; 2009.

5. Mladina R. A morphometric consideration of nasal septal deviations by people with paranasal complaints: a computed tomography study [letter]. Rhinology. 2003; 41(4):255. [PubMed: 14750356]

6. Rao JJ, Kumar ECV, Babu KR, Chowdary VS, Singh J, Rangamani SV. Classification of nasal septal deviations—relation to sinonasal pathology. Indian J Otolaryngol Head Neck Surg. 2005; 57(3):199–201. [PubMed: 23120171]

7. Guyuron B, Uzzo CD, Scull H. A practical classification of septonasal deviation and an effective guide to septal surgery. Plast Reconstr Surg. 1999; 104(7):2202–2212. [PubMed: 11149789]

8. Jin HR, Lee JY, Jung WJ. New description method and classification system for septal deviation. J Rhinol. 2007; 14(1):27–31.

9. Baumann I, Baumann H. A new classification of septal deviations. Rhinology. 2007; 45(3):220–223. [PubMed: 17956023]

10. Rohrich RJ, Gunter JP, Deuber MA, Adams WP. The deviated nose: optimizing results using a simplified classification and algorithmic approach. Plast Reconstr Surg. 2002; 110(6):1509–1525. [PubMed: 12409771]

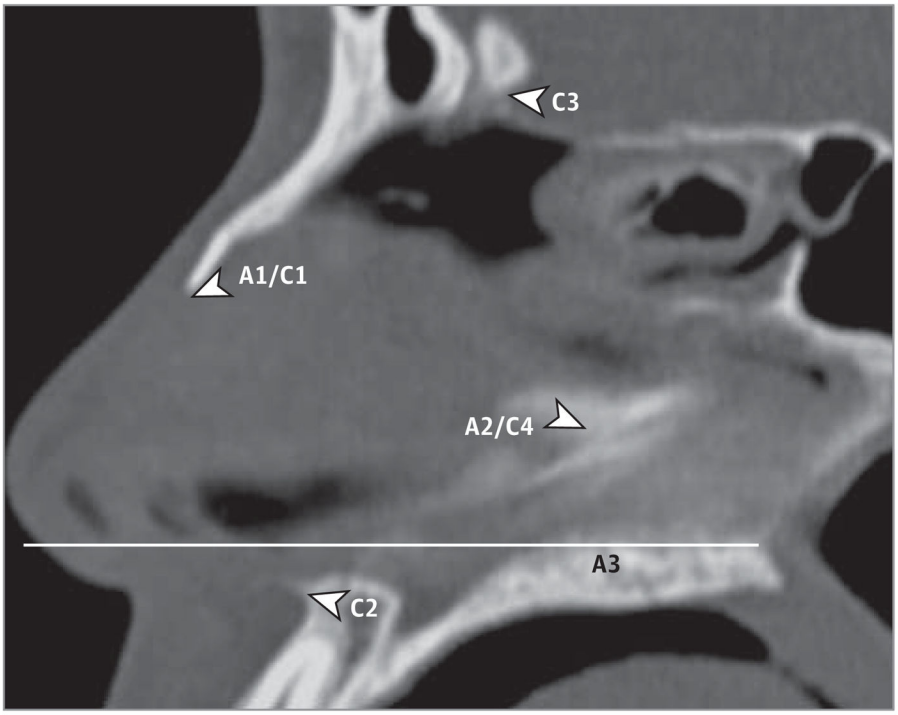


**Figure 1.**

Example of Sagittal Computed Tomographic Image Used for Axial and Coronal Landmark-Based Image Selection

Axial (A) and coronal (C) image sections were selected based on these respective points. A1/C1, anterior point of nasal bone; A2/C4, perpendicular plate–vomer junction; C2, anterior nasal spine; C3, crista galli; and A3, halfway point.

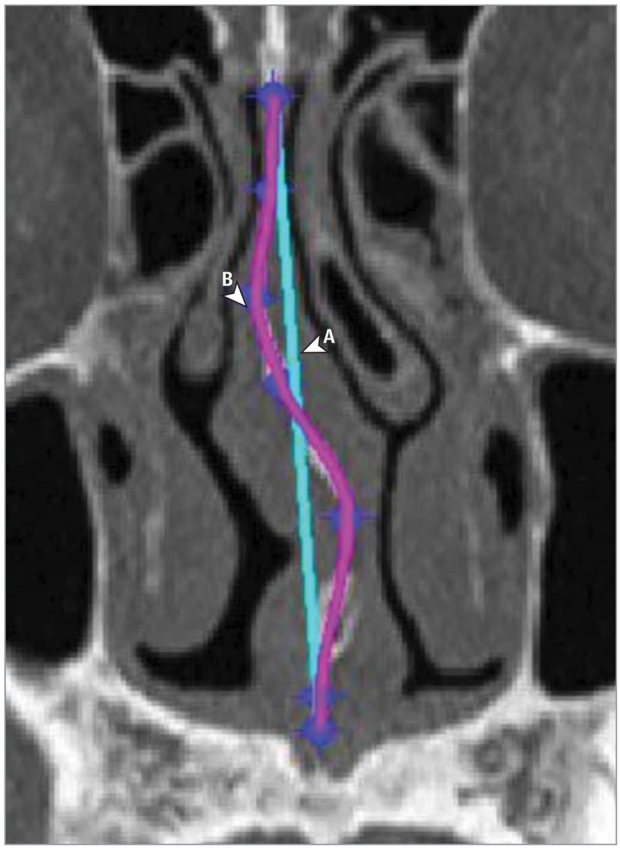


**Figure 2.**
Sample MATLAB Output From Analyzed Image
A portion of a coronal section computed tomographic scan is shown. A, Straight line representing the theoretical straight septum. B, Tracing of deviated septum fit to a polynomial curve. The area under the curve B to line A is the deviation area.

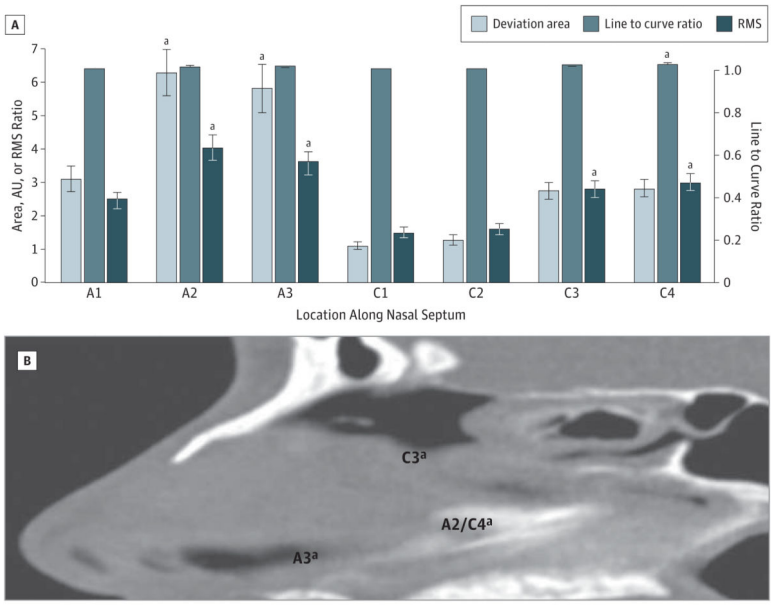


**Figure 3.**

Regions of Maximal Septal Deviation

A, Deviation area, line to curve ratio, and root mean square (RMS) values by location along the nasal septum. A1/C1 indicates anterior tip of nasal bone; A2/C4, perpendicular plate–vomer junction; A3, halfway point; AU, arbitrary units; C2, anterior nasal spine; and C3, crista galli. B, Sagittal computed tomographic scan showing areas of septal deviation with significantly increased RMS values. [a]$P < .05$.